To appear in the Astrophysical Journal
Preprint typeset using LaTeX style emulateapj v. 04/03/99

SENSITIVE RADIO OBSERVATIONS OF HIGH REDSHIFT DUSTY QSOS

M. S. Yun[1], C. L. Carilli[1], R. Kawabe[2], Y. Tutui[3], K. Kohno[2], & K. Ohta[4]

To appear in the Astrophysical Journal

ABSTRACT

We present sensitive radio continuum imaging at 1.4 GHz and 4.9 GHz of seven high redshift QSOs selected for having a 240 GHz continuum detection, which is thought to be thermal dust emission. We detect radio continuum emission from four of the sources: BRI 0952−0115, BR 1202−0725, LBQS 1230+1627B, and BRI 1335−0417. The radio source in BR 1202−0725 is resolved into two components, coincident with the double mm and CO sources. We compare the results at 1.4 GHz and 240 GHz to empirical and semi-analytic spectral models based on star forming galaxies at low redshift. The radio-to-submm spectral energy distribution for BR 1202−0725, LBQS 1230+1627B, and BRI 1335−0417 are consistent with that expected for a massive starburst galaxy, with implied massive star formation rates of order 10^3 $M_\odot$ year^{-1} (without correcting for possible amplification by gravitational lensing). The radio-to-submm spectral energy distribution for BRI 0952−0115 suggests a low-luminosity radio jet source driven by the AGN.

Subject headings: radio continuum: galaxies — infrared: galaxies — galaxies: starburst — galaxies: evolution — quasars: individual (BRI 0952−0115, BR 1033−0327, BR 1117−1329, & BR 1144−0723, BR 1202−0725, LBQS 1230+1627B, BRI 1335−0417)

1. INTRODUCTION

Detecting submm thermal dust emission from objects at z ≥ 2 has revolutionized our understanding of galaxies at high redshift (McMahon et al. 1994, Hughes et al. 1998, Ivison et al. 1998a, Smail, Ivison, & Blain 1997, Barger et al. 1998, Eales et al. 1999). A number of these submm sources have also been detected in CO emission with implied molecular gas masses > 10^{10} $M_\odot$ (Brown & Vanden Bout 1991, Barvainis et al. 1994, Ohta et al. 1996, Omont et al. 1996a, Guilloteau et al. 1997, Frayer et al. 1998, 1999), and the large reservoirs of warm gas and dust in these systems have led to the hypothesis that these galaxies are starburst galaxies with massive star formation rates of order 10^3 $M_\odot$ year^{-1} (Hughes & Dunlop 1999, Lilly et al. 1999).

In their study of optically selected QSOs at z > 4 from the APM sample (McMahon 1991, Irwin, McMahon, & Hazard 1991), Omont et al. (1996b) detected 240 GHz continuum emission in 6 out of 16 QSO's. If the detected emission is due to dust in the quasar host systems, the implied dust masses are ≈ 10^8 $M_\odot$. Follow-up observations of these dust emitting QSOs have revealed CO emission in three cases so far, with implied molecular gas masses ≈ 10^{11} $M_\odot$ (Ohta et al. 1996, Omont et al. 1996a, Guilloteau et al. 1997,1999, Carilli, Menten, & Yun 1999). Omont et al. also point out that about half the dust emitting QSOs have broad absorption lines (BALs), again suggesting a gas rich environment. Omont et al. speculate that: "...such large amounts of dust [and gas] imply giant starbursts at z > 4, at least comparable to those found in the most hyperluminous IRAS galaxies...". However, evidence for active star formation in these sources remains circumstantial, primarily based on the presence of large gas reservoirs, and it remains possible that the dust is heated by the AGN, rather than by a starburst.

One possible method to investigate the nature of these high redshift dust-rich QSOs is sensitive radio continuum observations. A well studied phenomenon in nearby star forming galaxies is the radio-to-far IR correlation, i.e. the tight correlation found between radio continuum emission and thermal dust emission (Condon 1992, Helou & Bicay 1993). The standard explanation for the radio-to-far IR correlation involves relativistic electrons accelerated in supernova remnant shocks, and dust heated by the interstellar radiation field. Both quantities are then functions of the massive star formation rate (Condon 1992, Cram et al. 1998, Yun, Reddy, & Condon 1999, Gruppioni, Mignal, & Zamorani 1999), although the detailed physical processes giving rise to the tight correlation remain enigmatic.

An obvious difficulty in interpreting the radio and infrared emission from an AGN host system in terms of star formation activity is disentangling the contribution associated with the AGN activity. A relatively minute amount of dust ($10^{6-7}M_\odot$) heated by a luminous AGN can produce detectable levels of infrared and submm emission (e.g. Yun & Scoville 1998). Similarly, all AGNs are likely sources of radio emission at some level, and whether a particular QSO is a radio source is really a question on sensitivity. For example, a VLA 5 GHz radio continuum survey of 22 optically selected high redshift ($z > 3$) QSOs by Schneider et al. (1992) has produced only one detection above the 5σ limit of 0.2 mJy[5] while another VLA survey of Palomar Bright Quasar Survey sources at $0.02 < z < 2.1$ by Kellermann et al. (1989) has detected 96 out of 114 (84%)

[1]National Radio Astronomy Observatory, P.O. Box O, Socorro, NM, 87801.
[2]Nobeyama Radio Observatory, Nagano 384-1305, Japan.
[3]Institute of Astronomy, University of Tokyo, Mitaka, Tokyo 181-8588, Japan.
[4]Department of Astronomy, Kyoto University, Kyoto 606-8502, Japan.
[5]1 Jy = 10^{-26} W m^{-2} Hz^{-1}

at a similar limiting flux level. The actual mechanism for generating luminosity by an AGN is not understood well enough nor particularly relevant to warrant further discussions here. Given that radio luminosity of an AGN can span nearly ten orders of magnitude, whether the observed radio luminosity of a dusty QSO host system is even comparable to the value expected from the inferred star forming activity is our main interest.

In this paper we present sensitive radio continuum observations of the high redshift dust rich QSOs from the APM sample made with the Very Large Array (VLA) at 1.4 GHz and 4.9 GHz. For about half the sample, our observations are sensitive enough to detect the radio continuum associated with a starburst, as dictated by the dust continuum emission and the radio-to-far IR correlation. We find that three of the sources are consistent with the radio-to-far IR correlation for starburst galaxies while the radio emission in one of the sources is likely dominated by a low luminosity (FR I) radio jet driven by the AGN. We then examine whether other high redshift, dust rich AGN hosts from the literature also follow the radio-to-far IR correlation for starburst galaxies, and we compare these results to the low redshift ultraluminous IR galaxy and BAL QSO Mrk 231. We adopt $H_\circ = 75$ km s^{-1} Mpc^{-1} and $q_\circ = 0.5$.

2. OBSERVATIONS

The sources listed in Table 1 are from a sample of optically selected $z > 4$ QSOs from the APM survey (Irwin et al. 1991, McMahon 1991, Storrie-Lombardi et al. 1996). They are selected for their very red color and point-like appearance, with the idea that the red color is due to the Lyα forest or the Lyman break shifting into the optical band. An additional contribution to the red color may be dust obscuration within the host galaxies. Omont et al. (1996b) observed 16 of these sources at 240 GHz to sensitivity limits of 1.5 mJy or better using the bolometer array on IRAM 30-m telescope. They claim detections at $\geq 3\sigma$ for six sources. We also include the z=2.70 QSO LBQS 1230+1627B, which was detected at 240 GHz by Omont et al. among their low redshift weak emission line sample.

Observations were made with the VLA in the BnA and C configurations at 1.4 GHz and 4.9 GHz between 1998 and 1999. Data from the VLA archive were also examined in some cases to verify our results. Integration times were between 1 and 2 hours long, and a total bandwidth of 2 $\times$ 50 MHz and two circular polarizations were used. The absolute flux density scale was set using 3C 286 (15 Jy at 1.4 GHz and 7.5 Jy at 4.9 GHz). After normal calibration using VLA calibrators, the data on each source were edited and self-calibrated using standard methods for high dynamic range imaging (Perley 1999). Wide-field images encompassing the full primary beam were synthesized and deconvolved in order to mitigate image noise due to sidelobes from sources distributed throughout the array field of view. The final rms noise levels on the images and measured source flux density are listed in columns 5 and 6 in Table 1. In most cases the final image noise values are within a factor 2 of the expected theoretical limits. The radio spectral index for each detected source between 1.4 GHz and 4.9 GHz is listed in column 7 in Table 1. We define spectral index, α, in terms of frequency, ν, and the observed flux density, S_ν, as: $S_\nu \propto \nu^\alpha$.

3. RESULTS ON INDIVIDUAL SOURCES

3.1. *BRI 0952−0115*

This z = 4.43 QSO is the weakest of the claimed detections by Omont et al. (1996b) with $S_{240} = 2.8 \pm 0.6$ mJy. Guilloteau et al. (1999) have recently detected CO(5−4) emission from this QSO, confirming its gas and dust rich nature. The optical QSO is gravitationally lensed with a $1''$ separation (Omont et al. 1996b), but the radio and mm observations made thus far have not had sufficient resolution to separate the two images.

This source is clearly detected at both 1.4 GHz and 4.9 GHz. The source is not spatially resolved by our observation at $4.5''\times2.7''$ resolution, and the measured flux density is 460±40 μJy and 234±27 μJy at 1.4 GHz and 4.9 GHz, respectively. The radio spectral index between 1.4 and 4.9 GHz is -0.54 ± 0.11, which is slightly flatter than the typical value for a starburst system, $\alpha \approx -0.75 \pm 0.1$ (Condon 1992).

If this were a starburst system at z = 4.43, then the expected 1.4 GHz flux density extrapolated from the 240 GHz flux density would be 44 μJy – about 5 times smaller than the actual observed value. Similarly, the observed value for $\alpha_{1.4}^{350}$ is +0.57±0.05 while the predicted value for a starburst galaxy at that redshift is +0.99±0.1. Therefore this source has clear excess of radio emission compared with a normal starburst galaxy. The radio luminosity of this source is about 5 times that of the radio-loud elliptical galaxy M87, and places this source in the class of low luminosity (Fanaroff-Riley Class I) radio galaxies.

One way to reconcile the starburst hypothesis for driving the radio emission from this source is to assume that gravitational lensing preferentially amplifies the radio emission relative to the dust emission. It is well known that differential magnification by gravitational lensing can significantly alter the apparent SED (e.g. Granato et al. 1996, Blain 1999a). For a pure starburst system, however, the radio-to-submm flux ratio should be relatively unaffected by lensing since radio synchrotron and thermal dust emission should have similar spatial extents (Condon et al. 1991). Gravitational magnification is approximately inversely proportional to angular size, and a preferential amplification of radio emission is expected only if a compact radio nucleus is present. Several other sources discussed here may also be lensed, and these considerations should generally apply to the others as well.

3.2. *BR 1202−0725*

The z = 4.70 QSO BR 1202−0725 is the first high redshift QSO where thermal dust emission was detected with $S_{240} = 12.6\pm2.3$ mJy and $S_{350} = 49\pm5$ mJy, respectively (McMahon et al. 1994). This source has also been detected in multiple transitions of CO (Ohta et al. 1996, Omont et al. 1996a, Yun, Scoville, & Evans 1999). This source has the curious property that the optical QSO is a single source, but the mm continuum and the CO line observations show a double source with a separation of about $4''$ (Omont et al. 1996a, Guilloteau et al. 1999). This double morphology may indicate a pair of interacting objects separated by only about 20 kpc. Alternatively, this may be a gravitationally lensed source with one of the optical images obscured by intervening material (see below).

We have detected radio continuum emission from BR 1202−0725 with a total flux density of 240±35 μJy at 1.4 GHz. The low resolution image (Figure 1a; $\theta = 10.6'' \times 6.6''$) shows a slight extension of the source along the position angle of the mm continuum and CO sources. The high resolution image (Figure 1b; $\theta = 4.5'' \times 2.8''$) shows a double source with the same separation and position angle as the mm continuum and CO emitting sources. This source is also detected at 4.9 GHz with a total flux density of 141 ± 15 μJy (Figure 1c). The resulting 1.4 GHz to 4.9 GHz spectral index is -0.43 ± 0.14, which is flatter than expected for a starburst galaxy.

The observed value of $\alpha_{1.4}^{350}$ for the integrated flux density for BR 1202−0725 is +0.96±0.04, while the value predicted for a starburst galaxy at z = 4.70 is +1.03±0.1. Hence the 1.4 GHz-to-350 GHz spectral index is consistent with a massive starburst. This conclusion is somewhat inconsistent with the derived radio spectral index above. One possible explanation for this discrepancy is free-free absorption of the radio continuum emission, although the required emission measures are large ($\approx$ few$\times 10^8$ pc cm^{-6}). Alternatively, a flat spectrum radio AGN may be present, contributing significantly at 5 GHz, with steeper spectrum emission driven by star formation dominating at 1.4 GHz. This later alternative is admittedly *ad hoc*, but the situation is similar to what is seen in another AGN+starburst system, Mrk 231 (see below). Future radio continuum imaging at sub-arcsecond resolution may help resolving this issue for BR 1202−0725.

If the 1.4 GHz radio emission is driven by star formation, then the required star formation rate is very large, $\approx$ 2500 M$_\odot$ year^{-1} (using Eq. 1 of Carilli & Yun 1999). Again, given the differences among galaxies, a star formation rate derived in this way should be considered an order-of-magnitude estimate at best, and that the true star formation rate could be a factor few to ten times lower if the source is amplified by gravitational lensing.

BR 1202−0725 is found in a high density environment, and gravitational lensing may not be needed to explain the double radio and submm morphology. There is a Lyman-α emitting companion located 2.6″ northwest of the quasar (Hu et al. 1996), and a deep ground based K-band image and an HST I-band image by Hu et al. show a string of continuum emission extending over 4″ in the same direction. There is also a second galaxy located about 3.5″ to the southwest of the quasar (see their Fig. 2). One of the two radio continuum sources is coincident with the optical quasar while the second radio and submm source is very close to but not coincident with the Lyman-α companion. A possible faint K-band counterpart is visible in the image obtained by Hu et al., and the radio and submm source is probably also physically related to the Lyman-α source. Citing the close proximity ($\sim$ 20 kpc), Hu et al. suggested ionization of the Lyman-α companion by the quasar. However, external heating by the quasar can not explain the bright radio and submm emission in the companion. If powered internally by star formation instead, the star formation rate inferred from the Lyman-α luminosity is only about $10 M_\odot$ yr^{-1}, which is about two orders of magnitudes smaller than inferred from the submm luminosity. Similarly weak Lyman-α emission has been seen in other dusty high redshift submm sources such as [HR94] 10 (ERO J164502+4626.4, Hu & Ridgway 1994, Cimatti et al. 1998a, Dey et al. 1999) and SMM 02399−0136 (Ivison et al. 1998a). The $\alpha_{1.4}^{350}$ index for the companion alone is +1.06±0.07, consistent with the SED of a z=4.7 starburst system. In this scenario, the QSO is a flat spectrum radio source located within a massive starburst host while the companion is a second dust obscured starburst system.

3.3. *BRI 1335−0417*

The z = 4.40 QSO BRI 1335−0417 has been detected at 240 GHz by Omont et al. (1996b) with a flux density of 10.3±1.0 mJy and by Guilloteau et al. (1997) with a flux density of 5.6±1.1 mJy at 220 GHz. This difference in observed flux densities at these two close frequencies is consistent with a sharply rising submm spectral index (see Guilloteau et al. 1997). Given the large uncertainty in each of these measurements, however, we adopt a mean value of 8.0±2.5 mJy at 240 GHz with an uncertainty encompassing both measurements. Then the expected flux density at 350 GHz is 31±9 mJy. This source has also been detected in CO (5–4) emission by Guilloteau et al. (1997), and in the CO (2–1) transition by Carilli et al. (1999), with an inferred molecular gas mass of $\approx 10^{11} M_\odot$. Neither the CO nor the thermal dust emission is resolved at 1″ resolution.

The source BRI 1335−0417 is detected in the radio continuum at 1.4 GHz and 4.9 GHz with flux densities of 220±43 μJy and 76 ± 11 μJy, respectively. There is a possible confusing source about 15″ to the east of BRI 1335−0417 (see Carilli et al. 1999). The 1.4 GHz to 4.9 GHz spectral index is -0.85 ± 0.19, consistent with synchrotron emission from a starburst system. The observed value of $\alpha_{1.4}^{350}$ for BRI 1335−0417 is +0.90±0.07 while the value predicted for a starburst galaxy at z = 4.40 is +1.0±0.1. Hence, the radio synchrotron and mm dust emission from BRI 1335−0417 are consistent with a massive starburst. Like BR 1202−0725, the required massive star formation rate is very large, $\approx$ 2000 M$_\odot$ year^{-1}. Thus far there is no evidence for gravitational lensing in BRI 1335−0417.

3.4. *LBQS 1230+1627B*

This z = 2.70 QSO is one of the low redshift QSOs in the Omont et al. sample with a 240 GHz detection. Omont et al. included this QSO in their search because they postulated that weak emission lines are indications of a possible dusty environment. The reported 240 GHz flux is S_{240} = 7.5±1.4 mJy. The Plateau de Bure observations by Guilloteau et al. (1999) have confirmed this detection, but they recovered only 3.3±0.5 mJy of flux at 225 GHz. The 850 GHz flux density of 104 ± 21 mJy has also been reported by Benford et al. (1999), and its dusty nature appears secure. A previous search for radio continuum produced only a 3σ upper limit of 0.24 mJy at 8.4 GHz (Hooper et al. 1995).

This source is detected at both 1.4 GHz and 4.9 GHz with measured flux density of 210±50 μJy and 86±11 μJy, respectively. The derived radio spectral index $\alpha_{1.4}^{5} = -0.72 \pm 0.22$ is typical of synchrotron emission from a star forming galaxy. Adopting an average value of 5.0±1.5 mJy at 230 GHz, the derived $\alpha_{1.4}^{350}$ is +0.82±0.07, consistent within the uncertainty with the predicted value for a starburst at z = 2.70 of +0.71±0.10.

3.5. *BR 1033−0327, BR 1117−1329, & BR 1144−0723*

Along with BRI 0952−0115, these QSOs are the faintest sources detected by Omont et al. (1996b), with S_{240} between 3.5 mJy and 5.8 mJy. The z = 4.51 QSO BR 1033−0327 was detected at 375 GHz by Issak et al. (1994) at 12±4 mJy while the extrapolated 350 GHz flux from the 240 GHz is 14±4 mJy. The extrapolated 350 GHz flux for the other two sources are 16 mJy and 23 mJy, respectively. We do not detect these three sources at 1.4 GHz, with 4σ upper limits between 170 μJy and 300 μJy. If the 240 GHz detection is real, then the 4σ lower limits to $\alpha_{1.4}^{350}$ are $\approx +0.8$ while the predicted values are $+1.0\pm0.1$. Hence the lower limits to $\alpha_{1.4}^{350}$ we obtained are consistent with a starburst interpretation, although these limits by no means preclude dust heated by an AGN in these systems.

4. DISCUSSION

In the local universe, galaxies with a pronounced dust peak and large FIR luminosity ($\geq 10^{12} L_{\odot}$) are luminous starburst systems fueled by a massive concentration of gas, enshrouded in a thick dusty cocoon (see Sanders & Mirabel 1996 and references therein). The 240 GHz continuum emission detected by Omont et al. in these high redshift QSOs correspond to rest frame wavelengths of between 240 μm and 350 μm, near the peak of their FIR dust spectral energy distribution (SED). We first consider their large FIR luminosity in relation to the ultraluminous infrared galaxies in the local universe. Then we consider the clear presence of optical QSOs and the possible AGN contribution to the radio and dust continuum emission.

4.1. *Starburst in Dusty QSOs*

The dust emission associated with these high redshift QSOs may be reprocessed radiation from luminous starburst activity within their host galaxies is strongly suggested by the comparison of their radio to infrared SEDs with that of a starburst galaxy like M82 (see Figure 2). While there is a natural expectation of finding some radio continuum emission associated with AGN activity in these QSOs, detecting radio emission exactly at the level expected from the dust emission has to be entirely fortuitous. The fact that this trend is seen in three out of four QSOs detected at both radio and mm/submm wavelengths is probably not coincidental. Rather, finding these luminous high redshift QSOs associated with gas and dust-rich, massive starburst systems should have been expected since most models of cosmic star formation history and galaxy formation/evolution trying to account for the faint submm source counts require up to two orders of magnitude increase in comoving density of such systems at earlier epochs (Guiderdoni et al. 1998, Blain et al. 1999, Tan et al. 1999).

The results of our radio continuum study of high redshift dust emitting QSOs are summarized in Figure 3. This figure shows the values of $\alpha_{1.4}^{350}$ versus redshift for the seven sources discussed above. Also plotted are submm detected dust rich galaxies with a wide range of redshifts and four models for the evolution of $\alpha_{1.4}^{350}$ with redshift for starburst galaxies as given in Carilli & Yun (1999). Two of the models are semi-empirical, based on starburst galaxy relationships derived by Condon (1992), while two of the models are empirical, based on the observed spectra of the low redshift star forming galaxies Arp 220 and M82. The radio-to-submm SEDs for the three sources, BR 1202−0725, LBQS 1230+1627B, and BRI 1335−0417, are consistent, within the uncertainty and the range of the models, with starburst-driven radio synchrotron and mm dust emission, despite the obvious presence of an optical QSO. One source, BRI 0952−0115, shows clear excess radio emission over the expected from a starburst.

Omont et al. have claimed $\geq 3\sigma$ detection of thermal dust emission at 240 GHz in 6 out of 16 QSOs from the APM sample at z $\geq$ 4. Three of these sources have also been detected in CO emission, and Omont et al. point out that half the sources are BAL QSOs – a phenomenon that is typically anti-correlated with radio-loud QSOs (see Weymann 1997). Overall, the host galaxies of these QSOs appear to be extremely gas rich, leading Omont et al. (1996a) to speculate that these AGN are associated with starburst host galaxies. However, detecting millimeter continuum emission alone does not serve uniquely as an indicator of a gas- and dust-rich galaxy vigorously forming stars since the presence of a flat spectrum AGN can account for the mm/submm detection in some cases (e.g. B2 0902+34, see Yun & Scoville 1996, Downes et al. 1996). Relatively small amount of hot dust ($10^{6-7} M_{\odot}$) heated by an AGN can also produce elevated submm emission (Yun & Scoville 1998, Haas et al. 1998). The fact that six out of seven 240 GHz detected QSOs have the same characteristic radio-to-submm SED (including lower limits), consistent with that of a starburst galaxy argues that these QSOs reside in gas and dust rich host galaxies harboring a massive starburst. The gas depletion time scale is short, $\approx 10^8$ years, during which time a significant fraction of the stars in the host galaxy may be formed.

There is a considerable scatter in the data and models plotted in Figure 3, and this relation may only be used as gross redshift *indicator*. Understanding the nature of contributing physical causes may allow a more robust use of this relation. An obvious concern is the contribution from a radio AGN (i.e. a jet), and the presence of an energetically important AGN in general is discussed in greater detail below. The intrinsic scatter in the radio-to-FIR correlation is only about 0.25 in dex (see Condon 1992), much smaller than the scatter seen in Figure 3. The mean electron density, which is a function of the compactness of the starburst region and the intensity of the starburst activity, can produce a varying degree of free-free absorption of radio continuum (see Condon et al. 1991), and this largely accounts for the systematic difference between the empherical models based on "M82" and "Arp 220" in Figure 3. As discussed by Blain (1999b), dust temperature and emissivity can also introduce variations at the submm/FIR wavelengths that may contribute to the observed scatter. To produce a significant deviation from the ranges of models considered in Figure 3, however, dust temperature has to be exceptionally low ($\lesssim$ 20 K). The measured dust SEDs of infrared luminous galaxies in the local universe are consistently characterized by dust temperature in excess of 30 K (see Benford 1999, Lisenfeld et al. 1999), and the models seem quite robust when applied to actively star forming galaxies.

It is well known that the fraction of radio loud QSOs decreases from about 20% at z $\leq$ 2 to 5% at z $\geq$ 3 (McMahon 1991, Schneider et al. 1992, Schmidt et al. 1995). In

this case, "radio-loud" implies radio luminosity an order of magnitude or more larger than the values presented herein, indicative of a radio jet associated with the active nucleus. The importance of the observations presented here is that the flux density limits adequate to detect the synchrotron radio continuum emission associated with star formation have been reached at least for some sources. Hence we are potentially probing a new population of radio-emitting AGN host galaxies at high redshift.

4.2. *Presence of a Luminous AGN*

There are now more than a dozen high redshift sources where thermal dust emission is detected. Many of these sources exhibiting a value of $\alpha_{1.4}^{350}$ characteristic of a starburst, and they also show clear evidence for an AGN. One such source is the z = 2.28 gravitationally lensed hyperluminous infrared galaxy IRAS 10214+4724. Presence of a hidden QSO is evidenced by broad optical emission lines seen in scattered light (Lawrence et al. 1993, Jannuzi et al. 1994). A second source is the z = 2.903 submm galaxy SMM 02399−0136, which is the first submm identified luminous galaxy showing an AGN spectrum (Ivison et al. 1998a). The third is APM 08279+5255 at z = 3.87, which shows an optical BAL QSO spectrum (Irwin et al. 1998, Lewis et al. 1998, Hines et al. 1999). These sources have also been detected in CO emission and thus harbor large amounts of molecular gas (Brown & Vanden Bout 1991, Frayer et al. 1998, Downes et al. 1999).

The z = 2.558 BAL QSO H 1413+117 is another submm and CO source (Barvainis et al. 1992,1994), but its radio emission has a significant contribution from its radio jet (Kayser et al. 1990). Therefore it deviates significantly from the radio-submm relation for starburst galaxies as shown in Figure 3, similarly as BRI 0952−0115. Other submm detected radio galaxies and radio-loud QSOs such as 4C 41.17 at z = 3.80 (Dunlop et al. 1994, Hughes et al. 1997), 8C 1435+635 at z = 4.25 (Ivison 1995, Ivison et al. 1998b), MG 0414+0534 at z = 2.64 (Barvainis 1998), and MG 1019+0535 at z = 2.76 (Cimatti et al. 1998b) have comparable submm/IR luminosity, but their radio luminosity is 2-3 orders of magnitude larger. As a result, they deviate so much from the radio-submm relation as to drop completely below the ranges plotted in Figure 3.

While we have argued for active star formation in at least some of these systems, the question remains as to what degree the luminous AGN present in these dusty QSOs account for the radio and/or submm/IR luminosity. The answer to this question is difficult to obtain even for the ultraluminous infrared galaxies in the local universe (see reviews by Sanders [1999], Joseph [1999], and Genzel [1999] and references therein), and addressing this issue for the high redshift objects has to be even harder. Instead, an examination of a low redshift analog of a galaxy with a concurrent AGN plus starburst in the ultraluminous infrared galaxy Mrk 231 may provide a useful insight. Mrk 231 is the most luminous infrared source at z ≤ 0.2 (Sanders et al. 1988), with an infrared luminosity of 5×10^{12} h^{-2} $L_\odot$. This is within a factor of a few to ten of the high redshift dust emitting sources, and Mrk 231 has been called the nearest BAL QSO (Forster et al. 1995). About half of its 1.4 GHz radio emission comes from a parsec-scale radio jet (Ulvestad et al. 1999) while the other half is associated with a gas disk seen in CO emission and HI 21cm absorption on scales of 100 to 1000 pc (Bryant & Scoville 1996, Downes & Solomon 1998, Carilli et al. 1998). The thermal dust and non-thermal radio continuum emission from this disk is consistent with a massive starburst of 200 $M_\odot$ per year, and support for such a star forming disk in Mrk 231 comes from the tentative detection of supernova remnants (Taylor et al. 1999). Citing geometric and energetic reasons, Downes & Solomon (1998) have argued that the AGN and the starburst each account for about 1/2 of the total luminosity in Mrk 231. The radio flux density of Mrk 231 between 5 GHz and 110 GHz is a factor 3 higher than the starburst prediction (see Figure 2) due to the contribution from the radio jet. This component is free-free absorbed at lower frequencies, where the flux densities are more in-line with those expected for a starburst.

Mrk 231 is an illustrative example of a dusty QSO where an AGN may provide significant infrared and radio luminosity. It is the closest local analog of the dusty high redshift QSOs whose radio emission has been studied here, but it is not certain if Mrk 231 is representative of the dusty QSOs in the early epochs. Nevertheless, the properties of Mrk 231 are consistent with the sequence proposed by Sanders et al. (1988) in which merging galaxies evolve through a starburst phase, eventually becoming optical QSOs (see also Sanders & Mirabel 1996). The time scale for such evolution is of order a few$\times 10^8$ to 10^9 years. Sanders et al. propose that Mrk 231 represents a late stage in this process, namely the 'dust enshrouded QSO' stage. Based on their radio and mm properties, many dust emitting high redshift QSOs also appear to fall in this category although the required star formation rates are a factor of 5 to 10 larger than IR luminous galaxies at low redshift (in the absence of amplification by gravitational lensing). Clearly, deeper radio and mm observations at sub-arcsecond spatial resolution are required to test this hypothesis. Such observations will become possible with the upgraded VLA at cm wavelengths and with the future Atacama Large Millimeter Array in Chile.

Despite the large error bars associated with the data points and a significant spread among the models, the dusty AGNs (filled and empty circles) as a group may suggest a systematic deviation by about 0.2-0.3 from the radio-submm relation obeyed by the pure starburst systems (empty squares) in Figure 3. It is tempting to interpret this trend as a residual effect of energy input by an energetic AGN in some cases, similarly as in Mrk 231 and to a lesser degree as in H 1413+117 and BR 0952−0115. Better and additional data on the high redshift dust-rich sources identified by SCUBA as well as more refined models with improved understanding of the intrinsic scatter are needed to examine the validity of this possible trend in detail.

5. SUMMARY

The 1.4 and 4.9 GHz radio continuum emission is detected in four out of seven high redshift QSOs that had previously be detected in thermal dust emission at 240 GHz by Omont et al. (1996b). In three of the cases, the cm and mm emission are consistent with starburst activity. One of the QSOs clearly hosts a radio AGN. If the detected radio continuum is interpreted solely in terms of AGN activity instead, the observed luminosity being within a factor of 2 of the value inferred for starburst activity would

be fortuitous, although such a possibility cannot be ruled out.

The authors thank F. Owen, A. Blain, I. Robson, R. Ivison, and K. Menten for useful discussions. This research made use of the NASA/IPAC Extragalactic Data Base (NED) which is operated by the Jet propulsion Lab, Caltech, under contract with NASA. The National Radio Astronomy Observatory (NRAO) is a facility of the National Science Foundation, operated under cooperative agreement by Associated Universities, Inc.

REFERENCES

Barger, A.J., Cowie, L.L., Sanders, D.B., Fulton, E., Taniguchi, Y., Sato, Y., Kawabe, K., & Okuda, H. 1998, Nature, 394, 248
Barvainis, R., Antonucci, R., & Coleman, P. 1992, ApJ, 399, L19
Barvainis, R., Tacconi, L., Antonucci, R., Alloin, D., & Coleman, P. 1994, Nature, 371, 586
Barvainis, R. 1998, in *Highly Redshifted Radio Lines*, eds. Carilli, Radford, Menten, & Langston, (San Francisco: PASP), p. 40
Benford, D. J. 1999, PhD thesis, California Institute of Technology
Benford, D. J., Cox, P., Omont, A., Phillips, T. G., & McMahon, R. G. 1999, ApJ, submitted
Blain, A.W. 1998, MNRAS, 297, 511
Blain, A.W. 1999, MNRAS, 306, 669
Blain, A.W. 1999, MNRAS, sumitted
Blain, A.W., Smail, I., Ivison, R.J., & Kneib, J.-P. 1999, MNRAS, 302, 632
Brown, R. L., & Vanden Bout, P.A. 1991, AJ, 102, 1956
Bryant, P.M. & Scoville, N.Z. 1996, ApJ, 457, 678
Carilli, C.L., Wrobel, J.M., & Ulvestad, J.S. 1998, AJ, 115, 928
Carilli, C. L., & Yun, M. S. 1999, ApJ, 513, L13
Carilli, C. L., Menten, K.M. & Yun, M. S. 1999, ApJ, submitted
Cimatti, A., Andreani, P., Rottgering, H., & Tilanus, R. 1998a, Nature, 392, 895
Cimatti, A., Freudling, W. Rottgering, H. J. A., Ivison, R. J., & Mazzei, P. 1998b, A&A, 329, 399
Condon, J.J. 1992, ARAA, 30. 575
Condon, J.J., Huang, Z.-P., Yin, Q.F., & Thuan, T.X. 1991, ApJ 378, 65
Cram, L., Hopkins, A., Mobasher, B., & Rowan-Robinson, M. 1998, ApJ, 508, 155
Dey, A., Graham, J. R., Ivison, R. J., Smail, I., Wright, G. S., & Liu, M. C. 1999, ApJ, in press (astro-ph/9902044)
Downes, D., Solomon, P. M., Sanders, D. B., & Evans, A. S. 1996, A&A, 313, 91
Downes, D. & Solomon, P.M. 1998, ApJ, 507, 615
Downes, D., Neri, R., Wilklind, T., Wilner, D. J., & Shaver, P. A. 1999, ApJ, 513, 1
Dunlop, J. S., Hughes, D. H., Rawlings, S., Eales, S. A., & Ward, M. J. 1994, Nature, 370, 347
Eales, S., Lilly, S., Gear, W., Dunne, L., Bond, J.R., Hammer, F., Le Fevre, O., & Crampton, D. 1999, ApJ, 515, 518
Forster, K., Michael, R. R., & McCarthy, J. K. 1995, ApJ, 450, 74
Frayer, D. T., Ivison, R. J., Scoville, N. Z., Yun, M. S., Evans, A. S., Smail, I., Blain, A. W., & Kneib, J.-P. 1998, ApJ, 506, L7
Frayer, D. T., Ivison, R. J., Scoville, N. Z., Evans, A. S., Yun, M. S., Smail, I., Blain, A. W., & Kneib, J.-P. 1999, ApJ, 514, L13
Genzel, R. 1999, Ap&SS, in press
Granato, G. L., Danese, L., & Franceschini, A. 1996, ApJL, 460, L11
Gruppioni, C., Mignoli, M., & Zamorani, G. 1999, MNRAS, 304, 199
Guiderdoni, B., Hivon, E., Bouchet, R., & Maffei, B. 1998, MNRAS, 295, 877
Guilloteau, S., Omont, A., McMahon, R. G., Cox, P., & Petitjean, P. 1997, A&A, 328, L1
Guilloteau, S., Omont, A., McMahon, R. G., Cox, P., & Petitjean, P. 1999, A&A, submitted
Haas, M., Chini, R., Meisenheimer, K., Stickel, M., Lemke, D., Klaas, U., & Kreysa, E. 1998, ApJ, 503, L109
Helou, G. & Bicay, M. D. 1993, ApJ, 415, 93
Hines, D. C., Schmidt, G. D., & Smith, P. S. 1999, ApJ, 514, L91
Hooper, E. J., Impey, C. D., Foltz, C. B., & Hewett, P. C. 1995, ApJ, 445, 62
Hu, E. M., & Ridgway, S. E. 1994, AJ, 107, 1303
Hu, E. M., McMahon, R. G., & Egami, E. 1996, ApJ, 459, L53
Hughes, D. H., Dunlop, J. S., & Rawlings, S. 1997, MNRAS, 289, 766
Hughes, D. H., et al. 1998, Nature, 394, 241
Hughes, D. H. & Dunlop, J. S. 1999, in *Highly Redshifted Radio Lines*, eds. Carilli, Radford, Menten, & Langston, (San Francisco: PASP), p. 103
Irwin, M., McMahon, R. G., & Hazard, C. 1991, in *The Space Distribution of Quasars*, ed. D. Crampton, ASP Conference Series, Vol. 21, p.117
Irwin, M. J., Ibata, R. A., Lewis, G. F., & Totten, E. J. 1998, ApJ, 505, 529
Isaak, K. G., McMahon, R. G., Hills, R. E., & Withington, S. 1994, MNRAS, 269, L28
Ivison, R. J. 1995, MNRAS, 275, L33
Ivison, R. J., Smail, I., Le Borgne, J.-F., Blain, A. W., Kneib, J.-P., Bezecourt, J., Kerr, T. H., & Davies, J. K. 1998a, MNRAS, 298, 583
Ivison, R. J., Dunlop, J. S., Hughes, D. H., Archibald, E. N., Stevens, J. A. et al. 1998b, ApJ, 494, 211
Jannuzi, B. T., Elston, R., Schmidt, G. D., Smith, P. S., & Stockman, H. S. 1994, ApJ, 429, L49
Joseph, R. D. 1999, Ap&SS, in press
Kayser, R., Surdej, J., Condon, J. J., Kellermann, K. I., Magain, P., Remy, M., & Smette, A. 1990, ApJ, 364, 15
Kellermann, K. I., Sramek, R., Schmidt, M., Shaffer, D. B., & Green, R. 1989, AJ, 98, 1195
Lawrence, A., Rowan-Robinson, M., Oliver, S., Taylor, A., McMahon, R. G. et al. 1993, MNRAS, 260, 28
Lewis, G. F., Chapman, S. C., Ibata, R. A., Irwin, M. J., & Totten, E. J. 1998, ApJ, 505, L1
Lilly, S. J., Eales, S. A., Gear, W. K. P., Hammer, F., Le Fever, O., et al. 1999, ApJ, 518, 641
Lisenfeld, U., Isaak, K. G., & Hills, R. 1999, MNRAS, in press (astro-ph/9907035).
McMahon, R. G. 1991, in *The Space Distribution of Quasars*, ed. D. Crampton, ASP Conference Series, Vol. 21, p.129
McMahon, R. G., Omont, A., Bergeron, J., Kreysa, E., & Haslam, C. G. T. 1994, MNRAS, 267, L9
Ohta, K., Yamada, T., Nakanishi, K., Kohno, K., Akiyama, M., & Kawabe, R. 1996, Nature, 382, 426
Omont, A., Petitjean, P., Guilloteau, S., McMahon, R. G., Solomon, P. M., & Pecontal, E. 1996a, Nature, 382, 428
Omont, A., McMahon, R. G., Cox, P., Kreysa, E., Bergeron, J., Pajot, F., & Storrie-Lombardi, L. J. 1996b, A&A, 315, 1
Perley, R. A. 1999, in *Aperture Synthesis in Radio Astronomy II*, eds. G. Taylor, C. Carilli, & R. Perley, (San Francisco: PASP), in press.
Sanders, D. B. 1999, Ap&SS, in press
Sanders, D. B., Soifer, B. T., Elias, J. H., Madore, B. F., Matthews, K., Neugebauer, G., and Scoville, N. Z. 1988, ApJ, 325, 74
Sanders, D.B. & Mirabel, I. F. 1996, ARAA, 34, 749
Schmidt, M., van Gorkom, J. H., Schneider, D. P., & Gunn, J. E. 1995, AJ, 109, 473
Schneider, D. P., van Gorkom, J. H., Schmidt, M., & Gunn, J. E. 1992, AJ, 103, 1451
Smail, I., Ivison, R. J., & Blain, A. W. 1997, ApJ, 490, L5
Storrie-Lombardi, L. J., McMahon, R. G., Irwin, M. J., & Hazard, C. 1996, ApJ, 468, 121
Tan, J. C., Silk, J., & Balland, C. 1999, ApJ, in press (astro-ph/9904004)
Taylor, G. B., Silver, C. S., Ulvestad, J., & Carilli, C. L. 1999, ApJ, in press
Ulvestad, J., Wrobel, J., & Carilli, C. L. 1999, ApJ, 516, 127
Weymann, R., in *Mass Ejection from Active Galactic Nuclei*, ASP Conference Series, Vol. 128, eds. N. Arav, I. Shlosman, & J. Weymann (San Francisco: ASP), p. 3
Yun, M. S., & Scoville, N. Z. 1996, in *CO: 25 Years of Millimeter-wave Spectroscopy*, eds. W. B. Latter, S. Radford, P. R. Jewell, J. G. Mangum, & J. Bally (Dordrecht: Kluwer), p341
Yun, M. S., & Scoville, N. Z. 1998, ApJ, 507, 774
Yun, M. S., Scoville, N. Z., & Evans, A. A. 1999, in *Highly Redshifted Radio Lines*, eds. Carilli, Radford, Menten, & Langston, (San Francisco: PASP), p58
Yun, M. S., Reddy, N., & Condon, J. J. 1999, in preparation

FIG. 1.— (a) A low resolution 1.4 GHz image of the z = 4.70 QSO BR 1202−0725 made with the VLA. The angular resolution is $10.6'' \times 6.6''$ (FWHM, with major axis position angle = 90^o). The crosses show the positions of the mm continuum and CO sources by Omont et al. (1996b). The contour levels are: −70, 70, 105, 140, 175, 210, and 245 μJy beam^{-1}. (b) The same as 1a, but now at higher resolution: $4.5'' \times 2.8''$ (FWHM) with major axis position angle = 82°. The contour levels are −64, −32, 32, 64, 96, and 128 μJy beam^{-1}. The emission appears to be resolved into two separate sources roughly coincident with the positions of the two submm sources reported by Omont et al. The flux densities and J2000 positions of the two sources are: 70±35 μJy at $12^h\ 05^m\ 23.16^s$, $-07^o\ 42'\ 32.4''$ and 133±35 μJy at $12^h\ 05^m\ 23.02^s$, $-07^o\ 42'\ 29.8''$ with position uncertainties of $\pm\ 1''$. (c) A 4.9 GHz image of the z = 4.70 QSO BR 1202−0725 made with the VLA. The angular resolution is $16.2'' \times 7.2''$ (FWHM, with major axis position angle = -69^o). The contour levels are: −45, −30, 30, 45, 60, 75, 90, 105, 120, and 135 μJy beam^{-1}.

FIG. 2.— The spectral energy distribution of 1335−0415 (squares) and BR 1202−0725 (circles) are compared with that of the prototypical starburst galaxy M82. The vertical scale is set for the flux density of M82, and the SEDs for all other sources are normalized to M82 at the peak of their dust SED. The intrinsic 1.4 GHz luminosity (i.e. in the source rest frame) of BRI 1335−0415 and BR 1202−0725 are a factor 1500 or so higher than M82. The SED for Mrk 231, an ultraluminous infrared galaxy and the nearest BAL QSO, is shown (stars with an error bar) as an illustrative example of a dusty QSO hosting a radio AGN. It has about 100 times larger 1.4 GHz luminosity than M82, and its flat spectrum radio nucleus and a radio jet accounts for a systematic offset between 10^{10-11} Hz.

FIG. 3.— The data points show derived values of $\alpha_{1.4}^{350}$ versus redshift for the sources in Table 1, including 4σ lower limits. The lines are models derived for starburst galaxies from Carilli & Yun (1999). Two power-law models for $\alpha_{1.4}^{350}$ for star forming galaxies as a function of redshift are shown with a solid curve ($\alpha_{\rm submm} = +3.0$) and a short dashed curve ($\alpha_{\rm submm} = +3.5$). The assumed radio spectral index is −0.8. The dotted and long-dashed curves show the expected values of $\alpha_{1.4}^{350}$ versus redshift based on the observed SED of the star forming galaxies M82 and Arp 220, respectively. The Omont et al. sample QSOs and Mrk 231 are plotted as filled circles while the lower limits for the three undetected Omont et al. QSOs are shown as arrows. Dusty sources from the literature with clear evidence for an AGN are also plotted as empty circles while the sources without evidence for an AGN are plotted as empty squares.

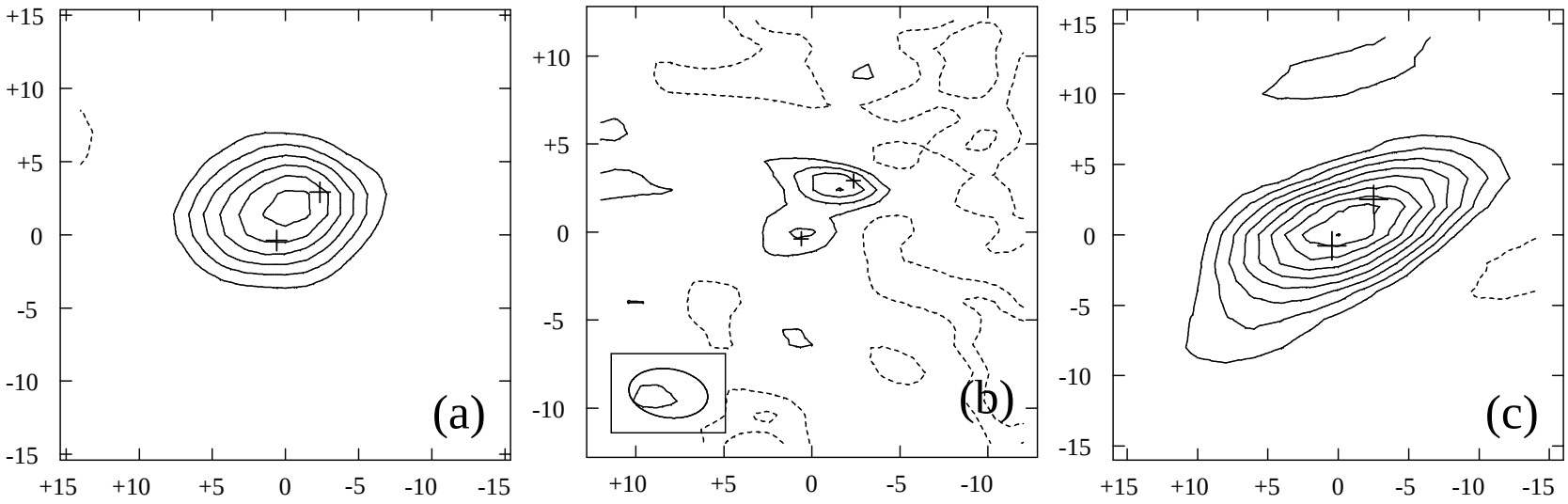
+15
+10
+5
0
-5
-10
-15
(a)
(b)
(c)

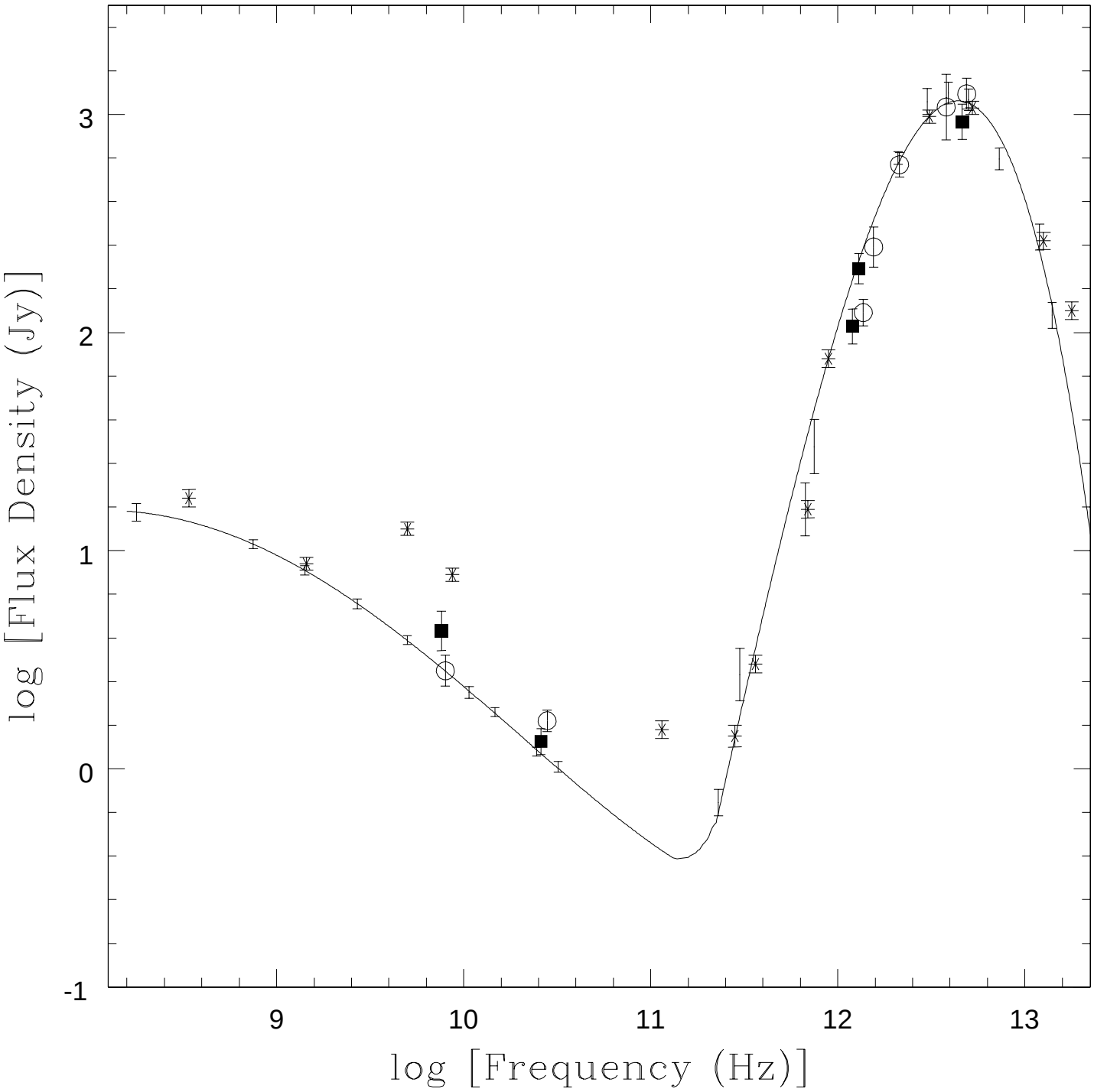
log [Flux Density (Jy)]
3
2
1
0
-1
9
10
11
12
13
log [Frequency (Hz)]

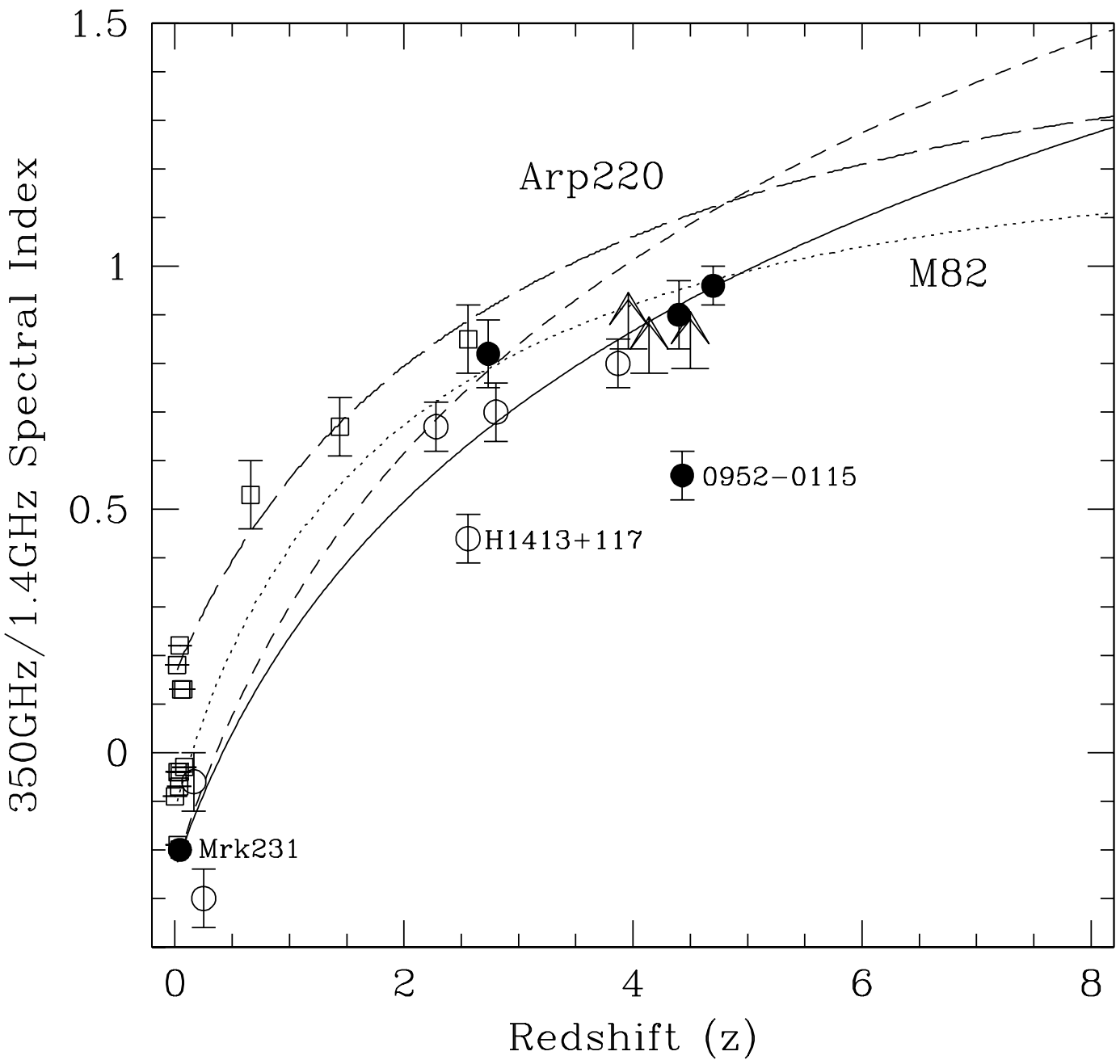
1.5
1
0.5
0
350GHz/1.4GHz Spectral Index
Arp220
M82
0952−0115
H1413+117
Mrk231
0
2
4
6
8
Redshift (z)

Table 1. Measured Fluxes and Radio-to-Submm Spectral Index

Source	z	RA (J2000)	Dec (J2000)	$S_{1.4GHz}$ (μJy)	S_{5GHz} (μJy)	$\alpha^5_{1.4}$(obs)	S_{350GHz}[a] (μJy)	$\alpha^{350}_{1.4}$(obs)[b]	$\alpha^{350}_{1.4}$(pred)[c]
BRI 0952−0115	4.43	$09^h55^m00^s.12$	$-01°30'06''.9$	460 ± 40	234 ± 27	-0.54 ± 0.11	11±3	0.57±0.05	0.99±0.10
BR 1033−0327	4.50	–	–	<170	–	–	14 ± 4	> 0.79	1.00±0.10
BR 1117−1329	3.96	–	–	<170	–	–	16±5	> 0.83	0.93±0.10
BR 1144−0723	4.14	–	–	< 300	–	–	23±6	> 0.78	0.95±0.10
BR 1202−0725	4.70	$12^h05^m23^s.09$	$-07°42'31''.1$	240 ± 35	141 ± 15	-0.43 ± 0.14	50±8	0.96±0.04	1.03±0.10
LBQS 1230+1627B	2.70	$12^h33^m10^s.32$	$+16°10'50''.8$	210 ± 50	86 ± 11	-0.72 ± 0.22	20±7	0.82±0.07	0.71±0.10
BRI 1335−0417	4.40	$13^h38^m03^s.44$	$-04°32'34''.1$	220 ± 43	76 ± 11	-0.85 ± 0.19	31±9	0.90±0.07	1.00±0.10

[a]Source flux density at 350 GHz (850 μm) is extrapolated from the 240 GHz flux density by Omont et al. (1996b) assuming a spectral index of +3.25. For BR 1033−0327 and BR 1202−0725, the 800 μm measurements by Isaak et al. (1994) are used instead.

[b]Observed 1.4 GHz to 350 GHz spectral index for each source or 4σ lower limits.

[c]Predicted value for a starburst galaxy using Eq. 3 of Carilli & Yun (1999). The uncertainty of 0.1 reflects a wide range of values predicted by the different models.

References. — (1) Omont et al. (1996b); (2) Issak et al. (1994); (3) McMahon et al. (1994); (4) Guilloteau et al. (1997); (5) Guilloteau et al. (1999)